Acta Cryst. (1998). A**54**, 922–933

Advances in Powder Diffraction Analysis

DANIEL LOUËR

Laboratoire de Chimie du Solide et Inorganique Moléculaire (UMR CNRS 6511), Groupe de Cristallochimie, Avenue du Général Leclerc, 35042 Rennes CEDEX, France. E-mail: daniel.louer@univ-rennes1.fr

(*Received 18 February 1998; accepted 26 May 1998*)

Abstract

Powder diffraction offers a wide spectrum of applications to solid-state scientists. The method traditionally used for phase analysis and the study of structural imperfections has benefited, in the last twenty years, from great advances in the instrumentation and computer-based approaches for pattern indexing and modelling. The factors at the origin of the metamorphosis of the method are presented. The major modern applications reported include quantitative analysis and the extraction of three-dimensional structural and microstructural properties. The use of pattern-fitting techniques for the characterization of the microstructure is discussed through applications to nanocrystalline materials. Remarkable results achieved in the solution of crystal structures are presented, as well as the impact in solid-state chemistry of powder crystallography, particularly for elucidating the crystal chemistry of families of compounds for which only powders are available. New strategies for solving the phase problem have been introduced and new classes of solids are being studied, such as drugs, coordination and organic compounds.

1. Introduction

Diffraction by polycrystalline solids is one of the most important analytical techniques available to materials scientists. Traditionally, the powder diffraction method has been used for phase identification and quantitative analysis, the measurement of precise unit-cell constants and the study of structure imperfections from line-broadening analysis. Diffraction theory by imperfect solids (crystallite size, lattice distortion, stacking faults) was well established half a century after the introduction of the powder method (see, for instance, Guinier, 1963) and many applications were reported in various fields of materials science, such as metallurgy, graphitic carbons and clay mineralogy. However, the full trace of a powder diffraction pattern contains a good deal of information, not only on the microstructure of a solid but also on its crystal structure. Although only one-dimensional data are available, there was a continuous effort to extract this important three-dimensional property for moderately complex structures. This became truly realistic from the late 1960s, following the advent of the Rietveld method (Rietveld, 1969) for the refinement of crystal structures from powder data. The dramatic transformation of the powder method was the consequence of several important developments in the methodology, often made possible by the power and availability of computers, and in the instrumentation using conventional X-rays, synchrotron X-rays or neutron radiation. All modern powder diffraction applications have benefited from these great advances, *e.g.* phase analysis, the investigation of structural imperfections and structural analysis. The powder method has been widely used since its introduction; however, its importance has been highlighted in recent times by its rôle in the characterization of high-T_c superconductors, fullerenes, zeolites, nanocrystalline solids and by the remarkable development of structure determination for compounds that can be obtained only in polycrystalline form. The method is nowadays used in various fields of materials science and chemistry, including the more recent applications to pharmaceutical compounds. Moreover, applications are not restricted to the analysis of solely one diffraction pattern registered at room temperature; they also extend to data collected under nonambient conditions (pressure, temperature, atmosphere) or in a dynamic mode, an area that continues to expand as more intense X-ray synchrotron and neutron sources became available and new detector technology is developed. The present article is not intended to review the details of the developments and all applications of modern

Daniel Louër received his doctorate in 1969 from the Faculty of Science of the University of Rennes, France, where he investigated deconvolution methods for instrumental correction and diffraction-line-broadening analysis. Since then, he has been working on powder-pattern indexing, instrumentation, profile-fitting techniques applied to microstructural studies, ab initio structure determination from powder data and temperature-dependent powder diffraction. He has been Directeur de Recherche at the Centre National de la Recherche Scientifique, France, since 1985. He was the recipient of the J. D. Hanawalt Powder Diffraction Award in 1992.

© 1998 International Union of Crystallography
Printed in Great Britain – all rights reserved

ISSN 0108-7673 © 1998

powder diffraction; interested readers should refer to the recent extended review *Powder Diffraction* by Langford & Louër (1996). The aim is to emphasize the factors at the origin of the renewal of the method and to describe the great activity in particular areas. This overview of modern powder diffraction is illustrated with examples, often studied simply with laboratory X-ray sources, selected to reflect the state of the art of the various facets of powder crystallography and its impact in materials and chemical sciences.

2. The line overlap problem: consequences and remedies

2.1. *Origin of diffraction-line overlap*

With respect to the spatially located single-crystal diffraction data, the principal limitation of powder data is the fact that the three-dimensional array of reciprocal nodes is rotationally projected onto one dimension, as a consequence of the random orientation of the crystallites constituting the sample. If crystallites are small and/or not perfect, the region of appreciable scattering is not concentrated at points of the reciprocal lattice but extends around the reciprocal nodes. In the powder diffraction pattern, only radial reciprocal distances d^* ($= 2\sin\theta/\lambda$) and the distribution of the intensity within diffraction lines are directly observed from the origin of the reciprocal space. The loss of information and its consequences that result from the collapse of the three-dimensional reciprocal space of the individual crystallites can be summarized as follows:

(i) The overlap of the diffraction lines can be accidental or exact. An exact superposition occurs when reciprocal nodes with different indices are located at the same distance from the origin of the reciprocal lattice. The observed diffraction line profile is then the summation of the projected intensity distribution associated with each node. There are two immediate consequences for analyses of structure and microstructure. Certain nonequivalent reflections exactly overlap, particularly for high crystal symmetry. It is then unclear how much each set of planes contributes to the observed lines. This reflection overlap, or information scrambling, is a serious obstacle which limits the size and complexity of structure that can confidently be investigated. In microstructural studies, only an average profile is observed for exactly overlapping lines. Therefore, only average crystallite shape, crystallite size and microdistortion can generally be extracted.

(ii) The degree of line overlap becomes increasingly severe as d^* increases, as shown by the total number of projected reciprocal-lattice nodes, which rises with d^{*3}. The density of lines is however lower at low Bragg angles, which is favourable for indexing powder diffraction patterns.

(iii) Diffraction line broadening contributes to the loss in resolution. It arises from the convolution between the instrumental $g(x)$ profile, including spectral dispersion, and the intrinsic $f(x)$ profile due to structural imperfections (crystallite size, strain, mistakes *etc.*).

(iv) An additional problem often arises from a preferred orientation of crystallites, particularly if they are markedly anisotropic. Although mathematical methods have been proposed to circumvent this problem (see, for example, Valvoda, 1992), it is recommended to reduce the effect prior to collecting powder data by an optimal specimen preparation (see, for instance, Jenkins & Snyder, 1996).

2.2. *Restoration of diffraction information*

Efforts to alleviate and overcome line overlap have been considerable from the late 1960s onwards. Modern powder crystallography has benefited from (i) an improved instrumental resolution, (ii) the introduction of pattern indexing methods for the geometrical reconstruction of the three-dimensional reciprocal lattice from one-dimensional data and (iii) the advent of fitting techniques to model the observed diffraction pattern. All these features have contributed to extending the limits of traditional applications, *e.g.* identification procedures, line-broadening analysis and quantitative analysis, and have been responsible for the emergence of new advanced applications, such as *ab initio* structure determination from powder diffraction data.

2.2.1. *Modelling of powder diffraction data*. Pattern modelling techniques constitute basic tools of modern powder diffraction. Two different approaches are currently applied, the pattern decomposition method, for which no structural information is required, and the Rietveld method, which includes the refinement of structure parameters. The procedure consists of fitting, usually with a least-squares refinement, a calculated model to the whole observed diffraction pattern. The calculated intensity $y(x_i)$ at point x_i is expressed as a function of the integrated intensity I_k of the reflections contained in the pattern and a normalized analytical function Φ is used to model the individual line profiles. It is given by

$$y_{\rm cal}(x_i) = \sum_k I_k \Phi(x_i - x_k) + b(x_i), \qquad (1)$$

where $b(x_i)$ is the intensity of the background and the sum is over all reflections contributing to the intensity at x_i. The method of least squares is then used to estimate the values of the adjustable parameters in the model. The most commonly used line-shape functions Φ are derived from the Gaussian (G) and the Lorentzian (L). The pseudo-Voigt function is the sum of G and L components, in which η is the mixing factor ($\eta = 1$ for L and 0 for G). The Pearson VII function is $(L)^m$, where the exponent m is the line-shape parameter ($m = 1$ for L and $m = \infty$ for G). The Voigt function is a convolu-

tion of L and G components whose limits of application are defined by the value of the shape parameter φ, defined as the ratio of the full width at half the peak intensity (FWHM) to the integral breadth (β), *i.e.* 0.6366 for L and 0.9394 for G. In practice, errors often arise from an unavoidable truncation of line tails, particularly for line profiles with Lorentzian trends (Toraya, 1985).

(*a*) *Pattern-decomposition method*. The purpose of pattern-decomposition techniques is to extract the profile parameters for individual Bragg components without reference to a structural model. They were introduced a few years after the advent of the Rietveld method (Taupin, 1973; Sonneveld & Visser, 1975). Line-profile parameters of interest extracted from the powder pattern are: peak position (2θ), full width at half-maximum intensity (FWHM), integral breadth (β), integral intensity (I), shape factor (η, m or φ) and some measure of line asymmetry. The method has greatly improved data reduction. Parameters are precisely determined and subtle differences detected in line shapes, especially line tails, are invaluable in determining microstructural properties.

In a related approach, aimed to extract the integrated intensity of *hkl* reflections for the entire pattern, peak positions are constrained by adjustable unit-cell parameters. If the space group is known, only intensities of allowed reflections are obtained. This approach produces a set of intensities up to an angular limit for all expected lines whatever the degree of line overlap. For exactly overlapping lines, an equipartition principle of the overall intensity is generally applied. After conversion to the structure-factor amplitude $|F_{\rm obs}|$, the set is used as input data for structure solution. Among the approaches most often employed are the Pawley technique (Pawley, 1981), based on a least-squares fitting of the pattern, and the Le Bail algorithm, derived from the procedure used by Rietveld [1969, equation (7)] for the partition of calculated intensities in the last stage of the refinement (Le Bail *et al.*, 1988). The Le Bail algorithm has been applied in a number of pattern-decomposition programs (see, for instance, Altomare, Burla *et al.*, 1995; Rius *et al.*, 1996). The last method is recognized as being very robust and stable, while the elimination of some instabilities in the Pawley approach needs some additional treatment (Jansen *et al.*, 1992; Sivia & David, 1994). For instance, an optimal estimate of the structure-factor amplitudes using a Bayesian procedure that circumvents the problems associated with negative intensities and minimizes the effects of Bragg reflection overlap has been described by Sivia & David (1994). Moreover, anisotropic thermal-expansion properties have also been exploited for the separation of overlapping Bragg reflections from powder data collected at different temperatures (Shankland, David & Sivia, 1997). It is important to stress here the crucial rôle of the extraction and precision of the structure-factor magnitude in structure solution. However, owing to the overlap of nonequivalent reflections, the set of extracted $|F_{\rm obs}|$ is always somewhat biased. To evaluate the amount of reliable intensity information extracted from a powder diffraction pattern, Altomare, Cascarano *et al.* (1995) have proposed an algorithm, based on a systematic study of line overlap (reflection proximity and individual FWHMs), to estimate the number of statistically independent reflections as a function of the limit of the selected angular range.

(*b*) *The Rietveld method*. Unlike the pattern-decomposition approach, in the Rietveld method the integral intensities I_k of the reflections are calculated from the atomic parameters in the model. Then equation (1) becomes

$$y_{\rm cal}(x_i) = S\sum_k m_k({\rm Lp})_k|F_k^2|P_k\Phi(x_i - x_k) + b(x_i), \quad (2)$$

where S is the scale factor, m_k the multiplicity of reflection k, $({\rm Lp})_k$ the Lorentz–polarization factor and P_k is the preferred-orientation correction function. To generate the full powder diffraction pattern, profile parameters to describe the width and shape of the diffracted reflections are also adjusted until a best fit of the calculated pattern to the observed pattern is obtained. For detailed information, the reader is referred to the book *The Rietveld Method* (Young, 1995).

A great deal of work has been devoted to modelling anisotropic line broadening arising from structural imperfections (crystallite size and distribution, microstrain, stacking faults). There are basic difficulties in modelling all kinds of anisotropic line broadening arising from such stuctural defects (Delhez *et al.*, 1995). Readers interested in the recommended approaches for treating anisotropic broadening are referred to the review by Le Bail (1992). However, even though the Rietveld method is widely used, the results of two Rietveld refinement 'round robins' organized by the Commission on Powder Diffraction (CPD) of the International Union of Crystallography clearly revealed a number of problems and led to recommendations for avoiding errors in atomic coordinates and their related standard deviations (Hill, 1992; Hill & Cranswick, 1994). As a consequence, the CPD has recently formulated a set of Rietveld refinement guidelines to help newcomers in the field (McCusker *et al.*, 1998).

2.2.2. *Geometric reconstruction of the reciprocal lattice*. Advances in powder-pattern indexing have greatly contributed to the development of modern powder diffraction. Indeed, pattern indexing is a prerequisite for most applications. The purpose of pattern indexing is the geometrical reconstruction of the three-dimensional reciprocal lattice from the radial distribution of d spacings. Considerable effort has been devoted over more than half a century to the solution of this basic problem of powder crystallography. The first important approach to the problem was reported by

Runge (1917), immediately after the introduction of the powder method. Major contributions in the field are due to de Wolff who emphasized the importance of data accuracy, clearly expressed in his quotation 'it (indexing) would be quite an easy puzzle if errors of measurements did not exist' (de Wolff, 1957). He also provided the means to discriminate the correct indexing from several possible mathematical solutions. To assess the reliability of an indexed pattern, he introduced a figure of merit (M_{20}), based both on the quality of the fit between observed and calculated d spacings and on the size of the unit cell (de Wolff, 1968). The idea was later used by Smith & Snyder (1979) for rating the quality of powder diffraction data, through a related parameter F_N. The higher the accuracy of data and the more complete the pattern, the larger are M_{20} and F_N. It is not possible to define an absolute value of M_{20} which guarantees correctness. However, a solution with M_{20} greater than 20 is usually correct, though this may not be true if there is a dominant zone in the pattern (see, for example, Louër, 1992). Different approaches to the indexing problem have been suggested and applied in computer programs. The Runge–Ito–de Wolff method is used in the program written by Visser (1969). A trial-and-error procedure, based on a permutation of Miller indices for low-angle lines, is used in the program *TREOR*90 (Werner *et al.*, 1985), while an exhaustive successive dichotomy algorithm has been preferred in *DICVOL*91 (Boultif & Louër, 1991). In an important paper, Shirley (1978) revealed to powder diffractionists the power of indexing methods. Their success rate is very high, provided that the quality of data is good enough. (The absolute error on peak position should be lower than $0.03°2\theta$.) Powder-pattern indexing methods, particular cases and data-collection requirements have been reviewed by Louër (1992). There is no particular problem with large unit-cell volumes as long as enough information is contained in the low-angle part of the pattern, *i.e.* dominant zones that occur when a crystal axis is significantly shorter than the two others are not present. Representative examples with large unit-cell volume, obtained with X-ray laboratory data, are monoclinic halotrycite [$V = 3152$ Å^3, $M_{20} = 15$, $F_{20} = 35(0.006, 98)$ (Werner, 1980)] and barium titanyl oxalate hydrate [$V = 2595$ Å^3, $M_{20} = 46$, $F_{20} = 107(0.0056, 50)$ (Louër *et al.*, 1990)]. Such results are encouraging for the study of certain categories of materials with large unit-cell volumes, such as molecular compounds and zeolites. The limits of applications and accuracy are extended with ultra-high-resolution X-ray synchrotron data, particularly for triclinic materials, *e.g.* the figures of merit for $Zr(OH)_2(NO_3)_2 \cdot 4.7H_2O$ were $M_{20} = 54$ and $F_{20} = 112(0.0059, 30)$ for data collected with conventional monochromatic Cu $K\alpha_1$ X-rays, while for data collected with the 2.3 HRPD at Daresbury SRS Laboratory they were $M_{20} = 295$ and $F_{20} = 635(0.0012, 26)$ (Cernik & Louër, 1993).

2.2.3. *High instrumental resolution*. The instrument and radiation used to collect powder data contribute to the line-overlap problem. The instrumental resolution is generally expressed as the full width at half-maximum FWHM (expressed in 2θ units) of a diffraction line from a standard material without intrinsic line broadening. The improvement of the instrumental resolution has been significant in recent times. A major advance was the advent of synchrotron X-rays with parallel-beam optics and a crystal analyser (Cox *et al.*, 1983), from which an ultra-high resolution of $\sim 0.01°2\theta$ can be achieved. Other advantages of synchrotron radiation are high intensity and tunable wavelength. These features have extended the limits of the complexity of structures that can be investigated from powders and have contributed to the emergence of resonant X-ray diffraction used to enhance the contrast between elements with similar atomic numbers (see, for example, Attfield, 1992). Nevertheless, most current applications, including line-broadening analysis, indexing and structure analyses are carried out from data collected with conventional X-ray sources. Parafocusing techniques are used with film focusing cameras and diffractometers based on Bragg–Brentano or transmission geometries. With an incident-beam monochromator, the component $K\alpha_2$ can be totally removed, giving high-resolution patterns with low background. With monochromatic radiation, the instrumental resolution function (IRF), FWHM *versus* 2θ, for the Bragg–Brentano geometry typically has a minimum of $\sim 0.06°2\theta$ at 40° and this value is doubled at about $130°2\theta$ (Louër & Langford, 1988). Detailed descriptions of instrument geometries used in modern powder diffraction have been reported by Parrish (1992) and Langford & Louër (1996). Moreover, the angular dependence of instrumental line shapes (breadth and line-shape factors) can be determined precisely from profile-fitting techniques applied to data from standard materials collected with the Bragg–Brentano geometry (Louër & Langford, 1988) or with the high-resolution powder diffraction optics used with synchrotron radiation (*e.g.* Cox, 1991; Langford *et al.*, 1991).

3. The analytical tool

Traditionally, X-ray powder diffraction has been a popular method for phase identification, often known as search/match, and quantitative analysis. Considerable improvements and new approaches have arisen from the methodology recently developed and from the general use of computer facilities. For instance, the identification of unknown materials or mixtures of phases has benefited from the revolution in storage media. The Powder Diffraction File (PDF) database from the International Centre for Diffraction Data (ICDD) contains data for over 100 000 substances stored on a CD-ROM, which is used in modern search/match programs. An important

innovation in search/match procedures is the use of the total diffraction pattern of the unknown substances, rather than simply the list of *d*'s and *I*'s. The method uses an interesting strategy for deciding whether or not the sample contains a particular PDF entry. Data for the latter are compared with regions of zero intensity in the pattern of the unknown sample (Caussin *et al.*, 1988). Interested readers are referred to the review by Langford & Louër (1996) and to the book by Jenkins & Snyder (1996).

In quantitative analyses, integrated line intensity and reference-intensity methods have been used for the determination of phase abundance in powder mixtures for many years (see, for example, Jenkins & Snyder, 1996). An extension of the Rietveld method is its use for quantitative analysis. Hill & Howard (1987) demonstrated that there is a very simple relationship between the individual scale factors S determined in a Rietveld refinement and the phase abundance of a multicomponent mixture. The weight fraction W of phase p is given by

$$W_p = S_p(ZMV)_p \Big/ \sum_i S_i(ZMV)_i, \qquad (3)$$

where Z, M and V are the number of formula units per unit cell, the mass of the formula unit and the unit-cell volume, respectively, and the summation is over all phases present. This approach based on the full diffraction profile provides numerous advantages over conventional quantitative analysis methods. In particular, it minimizes both the uncertainty in the derived phase abundances and the effects of preferred orientation, even though the correction of preferred orientation in the Rietveld method still needs some improvement (Valvoda, 1992). A number of applications have been reported. The procedure is of particular interest for the determination of the relative abundance of the constituents in rock samples (Hill *et al.*, 1993; Bish & Post, 1993). A representative example is the study of a standard granite, in which the results of the Rietveld refinement from X-ray and neutron diffraction data were compared with a normative calculation (Hill *et al.*, 1993). Fig. 1 shows the plot output from the Rietveld analysis of the four-phase mixture, as well as the good agreement between the quantitative analysis and the expected results.

4. Line-broadening analysis and microstructural properties

4.1. *Profile fitting and line-broadening analysis*

Microstructural imperfections (lattice distortion, stacking faults) and the small size of crystallites (*i.e.* domains over which diffraction is coherent) are usually extracted from the integral breadth or a Fourier analysis of individual diffraction-line profiles, for which theories are well established (see, for example, Guinier, 1963). In contrast with this direct approach of line-broadening interpretation, the calculation of line profiles on the basis of a physical model to be compared with the observed data has emerged in recent years. The modelling of diffraction effects due to a finite domain size with simple shapes is reasonably straightforward (see, for example, Langford & Louër, 1982), though crystallite-size distributions must be assumed to match with the observed diffraction patterns. The modelling of diffraction-line broadening due to distortion fields associated with lattice defects as dislocations has been investigated by Van Berkum *et al.* (1996). Nevertheless, with the advent of fitting techniques, analytical models of individual components can be extracted from clusters of reflections with reasonable accuracy, provided that the degree of line overlap is not too high. Indeed, line-broadening analysis is one of the most demanding applications of the powder method, in particular, line-profile tails must be perfectly modelled, which becomes increasingly unlikely in cases of severe line overlap. Propagation of errors in a Fourier approach can be serious, particularly those due to truncation (Delhez *et al.*, 1986). Consequently, most precise modern applications have resulted in the use of pattern-decomposition techniques for the study of high-symmetry compounds. These techniques have however contributed to an extension of line-broadening analysis to a greater number of reflections and a more detailed (three-dimensional) description of the microstructural properties has been reported in a few cases. These methods are usually applied to materials in which diffracting domains have sizes greater than a few nanometres (~50 Å). Two main approaches, combining pattern-decomposition and line-broadening analysis, have been described. They are based on:

(i) An interpretation of the integral breadth (Langford *et al.*, 1986). The use of the Voigt function, introduced in powder diffraction by Langford (1978) has greatly improved the analysis, particularly for correcting with accuracy the observed line breadths from the instrument contribution. For strain- and mistake-free materials, the corrected integral breadth β^*, expressed in reciprocal units, is related to an apparent size ε_β $(= \beta^{*-1})$, equivalent to the volume average of the thickness of the crystallites, measured in a direction of the scattering vector. The method requires that the observed (h), the instrumental (g) and the sample-dependent (f) line profiles are adequately represented by a Voigtian. An admirable account of the use of the method in extracting microstructural properties, as well as various applications, has been reported by Langford (1992).

(ii) A Fourier analysis, in which Fourier coefficients are interpreted in terms of microstructural properties (Warren, 1969). According to the Warren–Averbach–Bertaut procedure, the Fourier coefficients $C(n, l)$

[$= A(n, l) + iB(n, l)$, where n is the Fourier harmonic number and l the order of reflection] of the intrinsic $f(s)$ profile in reciprocal space can be expressed as the product of real order-independent size coefficients $A^S(n)$ and complex order-dependent, distortion coefficients $C^D(n, l)$ [$= A^D(n, l) + iB^D(n, l)$]. Considering only the cosine coefficients $A(n, l)$ [$= A^S(n)A^D(n, l)$] and a series expansion of $A^D(n, l)$, valid for small values of l and n, $A^S(n)$ and the microstrain $\langle e^2(n)\rangle$ can be readily separated, if at least two orders of a reflection are available, by means of the equation (Delhez & Mittemeijer, 1976)

$$A(n, l) = A^S(n) - A^S(n)2\pi^2 l^2 n^2 \langle e^2(n)\rangle . \qquad (4)$$

The initial slope of the size coefficients $A^S(n)$ *versus* n is a measure of an apparent size ε_F, defined as an area-weighted crystallite size (Bertaut, 1950). Another important result is that the Fourier coefficients $C(n)$ are

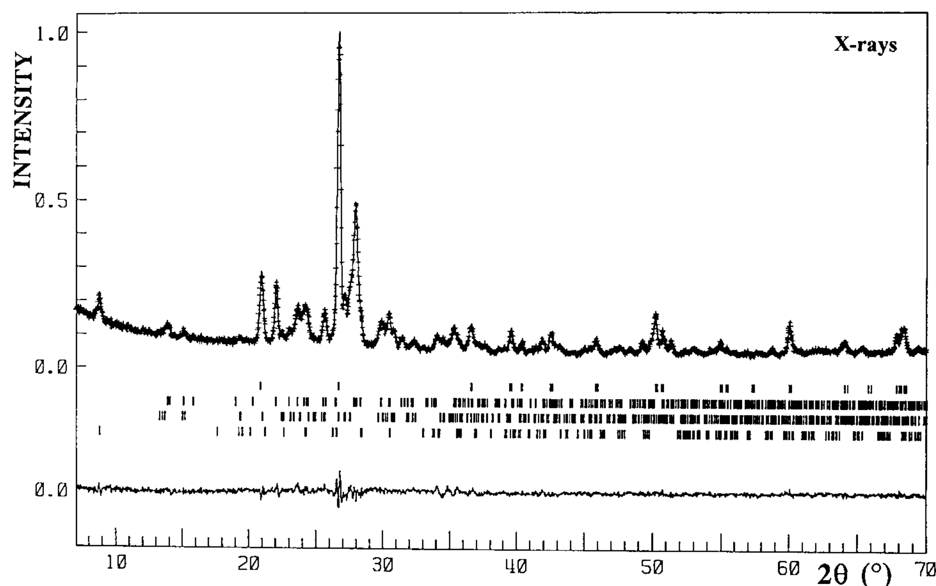

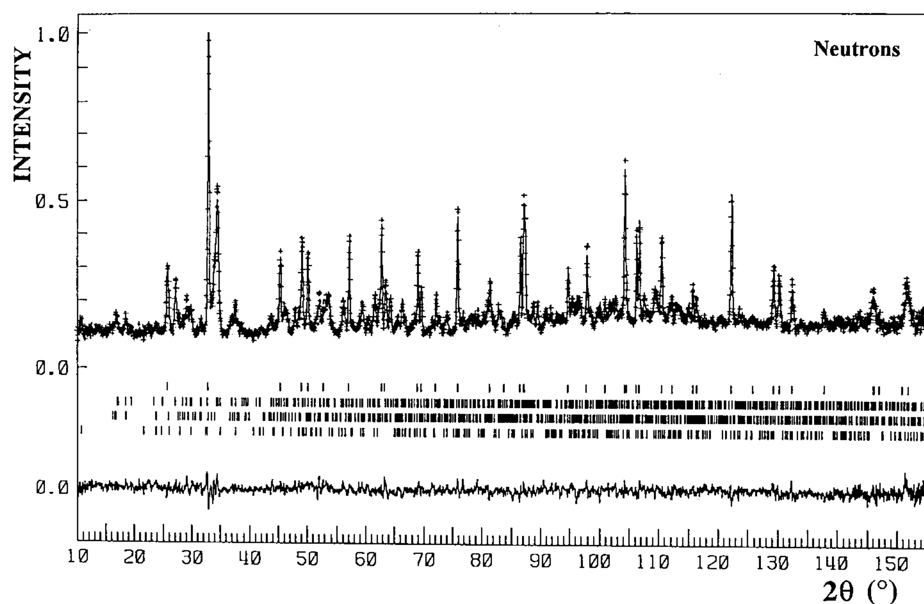

	X-rays	Norm	Neutrons
Quartz (wt %)	**24.6(6)**	**23.9**	**23.7(8)**
Plagioclase (wt %)	**43.2(10)**	**45.7**	**44.9(15)**
Microcline (wt %)	**27.2(7)**	**26.3**	**27.8(12)**
Biotite (wt %)	**5.0(3)**	**4.1**	**3.6(3)**

Fig. 1. Rietveld refinement plots for a standard granite sample obtained from X-ray diffraction data (Cu $K\alpha$) and neutron diffraction data (1.893 Å). The rows of vertical bars below the plots show the positions of the Bragg reflections for, from top to bottom, quartz, plagioclase, microcline and biotite. Phase abundances derived from X-rays and neutron data are compared to normative calculations (wt %). Reprinted with permission from Hill *et al.* (1993). Copyright (1993) Oxford University Press).

related to the integral breadth in reciprocal units β^* [$= \Delta s / \sum_n |C(n)|$, where Δs is the range of the line profile]. There is no assumption regarding the shape of the $f(s)$ profile and the method can then be used to obtain the integral breadth β_f^*, even in the case of asymmetry and super-Lorentzian line shape, provided that the deconvolution of observed profiles is correctly carried out. Several authors have combined fitting techniques with this procedure (*e.g.* Benedetti *et al.*, 1988; Louër & Audebrand, 1998). A related approach of Fourier analysis, assuming a Voigtian f profile, has also been reported (Balzar, 1992).

4.2. *Applications to nanocrystalline powders*

The number of applications of line-broadening analyses is considerable in various areas of materials science, *e.g.* thin films, metals and alloys, mineralogy, loose powders, ceramics *etc.* A representative example of the microstructural information contained in a powder diffraction pattern and extracted through profile-fitting techniques has been reported for several samples of hexagonal ZnO. The samples were prepared at low temperature from inorganic precursors with low thermal stability, $Zn_3(OH)_4(NO_3)_2$ (Louër *et al.*, 1983), $ZnC_2O_4 \cdot 2H_2O$ (Langford *et al.*, 1993), $Zn_5(OH)_6(CO_3)_2$ and $Zn(CH_3COO)_2 \cdot 2H_2O$ (Audebrand *et al.*, 1998). Physical parameters governing the synthesis were carefully monitored because they influence the microstructural properties. For ex-hydroxide-nitrate ZnO, there was no evidence of mistakes and crystallites had the form of a hexagonal prism with its axis parallel to the c direction of the unit cell, for which a cylinder is a reasonable approximation. In the case of a cylinder, the relation between the apparent size ε_β and the diameter D and height H depends on the angle φ_z, defining the direction of the diffraction vector with respect to the cylinder axis, and Φ [$= \tan^{-1}(D/H)$], the diagonal angle of the cylindrical shape. From Langford & Louër [1982, equations (10), (17) and (18)],

$$\varepsilon_\beta = \begin{cases} (D/\pi)\csc\varphi_z[8/3 + 2q\cos^{-1} q - (1/2q)\sin^{-1} q \\ \quad -(5/2)(1-q^2)^{1/2} + (1/3)(1-q^2)^{3/2}] \\ \qquad\qquad\qquad\qquad 0 \le \varphi_z \le \Phi \\ D\csc\varphi_z(8/3\pi - 1/4q) \qquad \Phi \le \varphi_z \le \pi/2, \end{cases} \tag{5}$$

where $q = H(\tan\varphi_z)/D$. Langford (1992) showed that these equations can be fitted by the method of least squares. Their general use in total-pattern-fitting algorithms to calculate integral breadths for crystallites with shapes varying from an acicular to a disk-like shape has also been discussed by Toraya (1995). A section through the cylinder obtained for ex-hydroxide-nitrate ZnO is displayed in Fig. 2(a). From the remarkable agreement between the experimental values of the actual thickness and the cylinder section [$\langle D\rangle = 180\,(10)$ Å, $\langle H\rangle = 270\,(60)$ Å], it is seen that this form clearly models satisfactorily the average shape of a crystallite (Langford *et al.*, 1993). From these results, a three-dimensional description of the diffracting domains has been obtained. It is then of interest to compare this result with a TEM analysis of the sample, as shown in Fig. 2(b). In the last case, only a two-dimensional view of the 'particles' has been obtained, showing, however, a good agreement between their average diameter and the mean diameter derived from X-ray diffraction-line-broadening analysis.

Similar crystallite shape and size analyses were repeated for ZnO samples obtained from the three other precursors. Additional important microstructural features about microstrains and stacking faults were also observed. The method was then used to study, on a nanometric scale, the early stages of crystallite growth from ZnO samples prepared *in situ* with a constant heating rate, from which interesting conclusions concerning growth mechanisms and precursor-dependent properties were established (Audebrand *et al.*, 1998). From a diffraction-line-broadening analysis of the successive patterns of ZnO, different crystallite growth régimes were identified with precursor-dependent linear relationships $\ln D$ (and H) *versus* T^{-1}. In order to determine the activation energy and the dimensionality of the crystallite-growth mechanisms, time-dependent X-ray diffraction studies were performed at selected temperatures, with an acquisition time of 600 s per pattern. Such results are invaluable in the study of the thermal behaviour of nanoscale powders, such as crystallite growth, annealing and crystallization phenomena. For this kind of application, conventional X-ray sources clearly have serious limitations. The use of high intensity available with synchrotron sources decreases considerably the time scale for collecting powder data.

5. *Ab initio* structure determination

5.1. *Methodology for structure solution from powder data*

With the advent of the powerful methods to recover the lattice constants of the three-dimensional reciprocal lattice, to extract integrated intensities and to refine crystal structure from powder data, the door has been opened to solve crystal structures. As a consequence, the field of structure solution has been an extremely active research area in recent years, including the development of software adapted to powder data. The procedure for solving structures from powder data is now well established and complex structures solved in this way are reported regularly. Although the difficulties in solving structures can have different origins, *e.g.* high-symmetry space-group ambiguity combined with a complex chemical formula and limited resolution data [*e.g.*

$C_{16}H_{22}N_6$, space group $P3$ (Ochando *et al.*, 1997)] and the size of the unit-cell volume {(*e.g.* 7471 Å^3 for $[(CH_3)_4N]_4Ge_4S_{10}$ (Pivan *et al.*, 1994)}, the number of atoms in the asymmetric unit is frequently used as a complexity indicator. Representative examples include structures with 29 atoms in the asymmetric unit, such as gallium phosphite $Ga_2(HPO_3)_3 \cdot 4H_2O$, space group $P2_1$ (Morris *et al.*, 1992), barium aluminium fluoride β-Ba_3AlF_9, space group $Pnc2$ (Le Bail, 1993), bismuth trifluoromethanesulfonate $Bi(H_2O)_4(OSO_2CF_3)_3$, space group $P2_1/c$ (Louër *et al.*, 1997), and also the structures of uranyl phosphonate $(UO_2)_3(HO_3PC_6H_5)_2 \cdot H_2O$, space group $P2_12_12_1$, with 50 non-H atoms in the asymmetric unit (Poojary *et al.*, 1996) and $La_3Ti_5Al_{15}O_{37}$, space group Cc, with 60 atoms in the asymmetric unit (Morris *et al.*, 1994). The most general strategy in structure analysis from high-quality powder diffraction data involves the following stages: (i) the determination of unit-cell constants from indexing methods and derivation of space groups; (ii) the extraction of the integrated intensities, which are converted to structure-factor magnitudes for use in (iii) methods of solving the phase problem; (iv) the refinement of the approximate structure model with the Rietveld method. An alternative strategy, useful for instance in the study of organic compounds, is to generate structure models with direct-space methods independently of the powder diffraction data, which are then selected from a direct comparison with the observed powder pattern. This approach avoids the critical step of extracting individual intensities by means of total-pattern-decomposition methods.

In earlier studies, only structure-factor magnitudes of unambiguously indexed reflections were used for structure solution with Patterson or direct methods. Representative examples include structures solved from conventional X-ray data, *e.g.* $(NH_4)_4[(MoO_2)_4O_3](C_4H_3O_5)_2 \cdot H_2O$ (120 $|F_{obs}|$) (Berg & Werner, 1977), $Zr(HPO_4)_2 \cdot H_2O$ (50 $|F_{obs}|$) (Rudolf & Clearfield, 1985), $KCaPO_4 \cdot H_2O$ (92 $|F_{obs}|$) (Louër *et al.*, 1988) and from synchrotron X-ray data, *e.g.* α-$CrPO_4$ (68 $|F_{obs}|$) (Attfield *et al.*, 1986). The introduction of total-pattern-decomposition techniques (Pawley and Le Bail methods) to extract integrated intensities automatically has transformed this procedure and all reflections up to an angular limit are used as input to a method for structure solution.

Although the traditional methods of solving the phase problem used with single-crystal data, *i.e.* the Patterson and direct methods, are generally applicable with powder data, considerable effort has been devoted to adapting these approaches to the powder case and to the introduction of a new methodology. Most of these developments in the solution of unknown crystal structures have been discussed in detail in recent reviews (McCusker, 1991; Cox, 1992; Cheetham, 1995; Langford

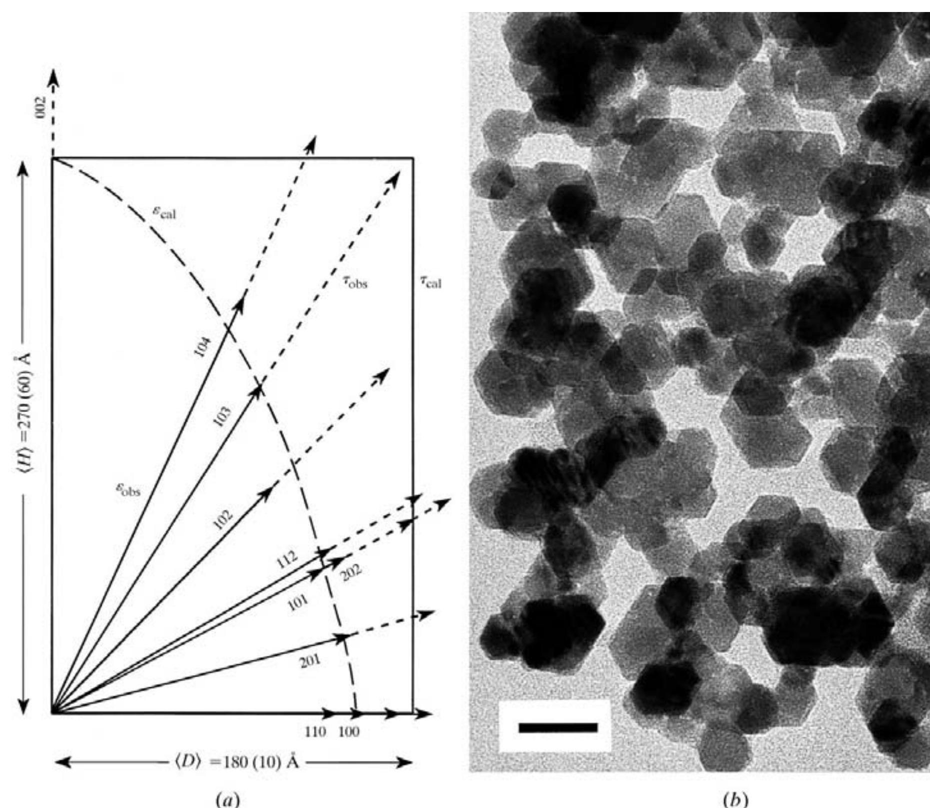

Fig. 2. (*a*) Representation of the 'average' (three-dimensional) cylinder used to model the shape of the crystallites of ex-hydroxide-nitrate ZnO. The lengths of the shorter arrows (full lines) are the observed apparent sizes (ε_{obs}) in the direction of the diffracting vectors; the actual observed sizes (τ_{obs}) are represented by the lengths of the higher arrows (dotted lines); the dotted curve is the loci of the calculated apparent sizes (from Langford *et al.*, 1993). (*b*) Transmission electron micrograph of ex-hydroxide-nitrate ZnO crystallites (bar is 200 Å).

& Louër, 1996; Giacovazzo, 1996; Harris & Tremayne, 1996; Gilmore, 1996; Poojary & Clearfield, 1997; Masciocchi & Sironi, 1997). The state of the art for some of these methods has been discussed more substantially, *e.g.* the entropy-maximization and likelihood-ranking method (Harris & Tremayne, 1996; Gilmore, 1996), direct methods (Giacovazzo, 1996), Monte Carlo methods (Harris & Tremayne, 1996) and simulated-annealing approaches (Newsam *et al.*, 1992). Methods adapted to low-resolution data have also been reported to assist structure determination, *e.g.* Patterson search algorithms using large known molecular fragments (Rius & Miravitlles, 1988) and multisolution direct methods (Rius *et al.*, 1995). Other direct-space methods have been applied in recent times, especially for handling powder data of organic materials. These are based on fitting a powder diffraction pattern generated from a trial structure model to the observed pattern. These new procedures include the application of a genetic algorithm (Shankland, David & Csoka, 1997; Harris *et al.*, 1998), the atom–atom potential method (Louër *et al.*, 1995), whose principles for crystal structure prediction by packing optimization have been reviewed by Dzyabchenko *et al.* (1996), and a method developed for the study of zeolite structures based on the generation of a large number of electron-density maps using random starting phases and structure-factor magnitudes derived from the extracted intensities. These are then subjected to a Fourier recycling procedure with a specialized topology search (McCusker *et al.*, 1996).

5.2. *The impact in solid-state chemistry*

The rapid growth of *ab initio* structure determinations reported in various fields of solid-state chemistry is evidence of the importance of this development in the powder diffraction method. Some hundreds of structures have already been solved from powder data. These have been concerned with inorganic, organometallic, organic and coordination compounds. Several classes of compounds, for which the growth of single crystals is difficult or impossible, have greatly benefited from this progress in powder crystallography. Representative examples are fullerene derivatives (*e.g.* David *et al.*, 1991; Dinnebier *et al.*, 1995) and synthetic zeolite molecular sieves, *e.g.* $(AlPO_4)_3 \cdot (CH_3)_4NOH$ (Rudolf *et al.*, 1986) and $(Si_{64}O_{128}) \cdot 4C_{10}H_{17}N$ (McCusker, 1988). Structures of related microporous materials have also been reported. For instance, the structure of the noncentrosymmetric cubic compound $[(CH_3)_4N]_4Ge_4S_{10}$ [$a = 19.5490\,(4)$ Å, space group $P\bar{4}3n$] was solved from data collected with a conventional X-ray source (Pivan *et al.*, 1994). A partial model was derived by means of direct methods from a total of 436 structure factors. The structure model was completed from a difference-Fourier map generated from 958 structure-factor amplitudes. This structure model with 15 atoms in the asymmetric unit and 37 variables was refined by the Rietveld method ($R_F = 6\%$, $R_{wp} = 12\%$). The structure consists of isolated thioanions $Ge_4S_{10}^{4-}$, formed from the condensation of four GeS_4 tetrahedra sharing apices, with tetrahedral $(CH_3)_4N^+$ cations as positive counterparts. Owing to the high volume of the unit cell (7471 Å^3), the packing of the structure is not easy to describe. However, the description can be simplified by considering the quasiperfect f.c.c. arrangement of the apical S atoms of the $Ge_4S_{10}^{4-}$ thioanion. In this description, all octahedral voids are filled by the $(CH_3)_4N^+$ ions, while only one-eighth of the tetrahedral voids are occupied by the adamantine-like Ge_4S_6 moieties (Fig. 3).

To illustrate the great impact of structure determination from powder data in solid-state chemistry and structural chemistry of families of compounds, which were ignored until recent years because only powder samples were available, two local examples will be described briefly. All these studies were based on data collected with a conventional monochromatic X-ray source. They show that, similar to the contribution of structure determination from single-crystal diffraction data from the 1950s onwards in the progress of modern chemistry, powder crystallography now plays a significant rôle in the structural characterization of powder materials. For instance, the chemistry of uranium phosphates has been transformed due to the *ab initio* structure determination of three major polycrystalline phases: $U(UO_2)(PO_4)_2$, a mixed-valence compound,

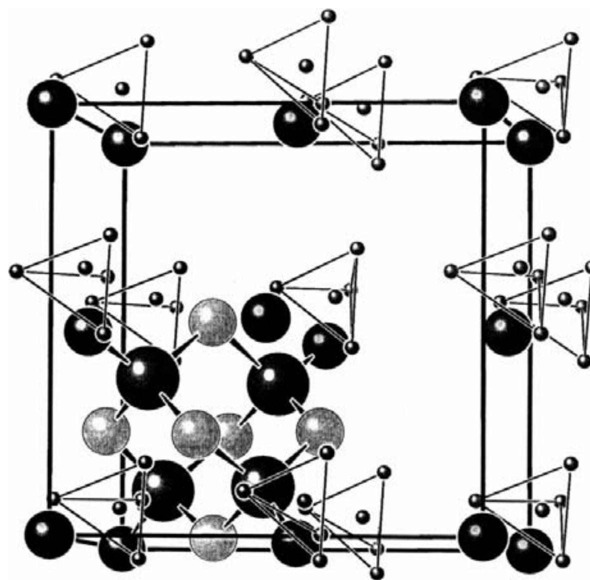

Fig. 3. Crystal structure of $[(CH_3)_4N]_4Ge_4S_{10}$ with a high cubic cell volume (7471 Å^3) solved *ab initio* from powder diffraction data: perspective view of one subcell ($a' = a/2$) showing the quasiperfect f.c.c. arrangement of the apical S atoms (in black) of the $Ge_4S_{10}^{4-}$ thioanions, the tetrahedral $(CH_3)_4N^+$ cations are located approximately in the octahedral sites and the Ge_4S_6 unit in one tetrahedral site (from Pivan *et al.*, 1994).

$U_2O(PO_4)_2$ and $UXPO_4 \cdot 2H_2O$ (X = Cl, Br) (Bénard-Rocherullé, Louër *et al.*, 1997, and references therein).

(*a*) *Low-dimensional zirconium hydroxide nitrates.* Zirconium is known to form a large number of hydroxy salts. This is observed, for instance, for nitrate-based phases, for which a number of compounds have been identified from their powder diffraction pattern and further characterized from the indexing of their powder diffraction pattern. Zirconium hydroxide nitrates are polycrystalline and the crystal structure of four varieties has been solved from powder data (Bénard-Rocherullé, Rius & Louër, 1997, and references therein). These powder diffraction studies have shed light on the crystal chemistry of this family of compounds. All structures are built from edge-sharing ZrO_8 trigonal dodecahedra. In $[Zr(OH)_2(NO_3)_2] \cdot 4.7H_2O$, they form infinite isolated chains considered as linear macrocations $[Zr(OH)_2(NO_3)(H_2O)_2]_n^{n+}$, which are balanced by an equivalent amount of nitrate anions. Water molecules are located between the chains. Neutral zigzag chains $[Zr(OH)_2(NO_3)_2(H_2O)]_n$ are observed in the two structures of $[Zr(OH)_2(NO_3)_2] \cdot 1.65H_2O$ and β-$[Zr(OH)_2(NO_3)_2] \cdot H_2O$, while 'free' water molecules are located between them. Unlike these three one-dimensional structures, the structure of $Zr(OH)_3NO_3$ is surprisingly two-dimensional. It consists of neutral layers formed from the condensation of chains already observed in the other basic salts. These results reflect the complexity of the crystal chemistry of this family of zirconium phases. It is a neat illustration of the use of recent advances in structure determination from powder data to elucidate the crystal chemistry of series of compounds.

(*b*) *Piracetam, a drug polymorph with a 2 h lifetime.* Drug substances offer new challenges to the powder diffraction technique. In general, they are essentially based on organic components and their patterns exhibit the familiar rapid fall-off in intensity with increasing Bragg angle. With Cu $K\alpha$ radiation, the intensity of the reflections usually vanishes around $60°2\theta$. To improve counting statistics, particularly at high angles, an optimized procedure using a systematic variable-counting-time strategy that is inversely proportional to the decrease in line-profile intensity (Madsen & Hill, 1994) was applied in the structure determination with direct methods of the drug chlorothiazide from synchrotron X-ray diffraction data (Shankland, David & Sivia, 1997). For the structure solution of a metastable polymorph of piracetam, counting statistics at high angles were enhanced by using a position-sensitive detector (CPS120, INEL) incorporated in a Debye–Scherrer set-up, operating with monochromatic Cu $K\alpha_1$ radiation (Louër *et al.*, 1995). Piracetam [(2-oxo-1-pyrrolidinyl)-acetamide], $C_6H_{10}N_2O_2$, is a drug used in human therapeutics, for which three polymorphs have been identified. The structure of two of them was solved from single-crystal data. The third polymorph, metastable at room temperature, is obtained as a result of phase transformation upon heating at 408 K one of the stable phases. At room temperature, this phase transforms within 2 h into one of the stable phases (Céolin *et al.*, 1996). Unit-cell determination (V = 723 Å^3, monoclinic, space group $P2_1/n$) was carried out with *DICVOL*91. An attempt to solve the structure by direct methods was unsuccessful. Therefore, a computational study of the piracetam polymorphs based on minimization of the crystal-lattice potential energy, calculated with semi-empirical atom–atom potentials, was used for structure solution. In this method introduced by Kitaigorodsky (1973), structure models are postulated independently of the powder diffraction data. The method assumes that the molecule conformation is known and it involves the search for the most favourable crystal packing constrained by the known unit-cell dimensions and space groups. The same molecular conformation as observed in the structure of the two stable phases of piracetam was expected to occur in the metastable phase. As a result of packing calculations, two distinct minima of crystal-lattice potential energy with $E_r = -100.78$ and -87.29 kJ mol^{-1} were obtained. The acceptance of only one of the models was based on the agreement between calculated and observed patterns. The atomic coordinates of the ten non-H atoms were refined with the Rietveld method. The ten H-atom positions were calculated and introduced in the last calculation, but not refined. The final R factors were $R_B = 0.04$ and $R_{wp} = 0.04$.

6. Concluding remarks

The above discussion and illustrations have demonstrated that the last two decades have been a very exciting time in the field of powder diffraction. The key to the successes remains the quality of the experiments. Ultra-high-resolution instruments and high-intensity sources of radiation available with synchrotron X-ray sources offer powerful facilities, which contribute to extend considerably the complexity of the problems that can be solved from powder diffraction. Although the precision of X-ray Rietveld refinements are often modest, in particular for materials with light atoms, the use of combined X-ray and neutron diffraction data contributes to enhanced accuracy. *In situ* non-ambient powder diffraction (see Langford & Louër, 1996), not covered in this overview of the powder method, has also greatly benefited from the new methodology. It is probably the *real world* of powder diffraction applications, since solid-state transformations due to external constraints (temperature, pressure, atmosphere *etc.*) usually give powders. The application of all modern powder diffraction techniques, *e.g.* structure and microstructure analyses, to data collected at non-ambient conditions leads to a better knowledge of the behaviour of materials under conditioned environments.

Representative examples are applications to industrial solid-state materials (Barnes *et al.*, 1996), electrochemical materials (Chabre & Pannetier, 1995), minerals (Artioli, 1997) and combinations of experiments such as powder diffraction, small-angle X-ray scattering and X-ray absorption spectrocopy (Cheetham & Mellot, 1997). All the methods described in this article will have a significant rôle to play in the future. This will be enhanced by the use of intense high-resolution sources, such as dedicated synchrotron rings and neutron time-of-flight sources. For instance, instrumental resolutions lower than $0.01^\circ 2\theta$ have already been reported at the ESRF with highly crystalline powders. Applications are also greatly facilitated by the development of software designed to handle powder data in a systematic way, similar to the usual analysis of single-crystal data. Moreover, the new direct-space methods and computer-simulation approaches for crystal-structure predictions should also have a great impact in the study of certain classes of solids, *e.g.* drugs and organic materials.

References

Altomare, A., Burla, M. C., Cascarano, G., Giacovazzo, C., Guagliardi, A., Moliterni, A. G. G. & Polidori, G. (1995). *J. Appl. Cryst.* **28**, 842–846.

Altomare, A., Cascarano, G., Giacovazzo, C., Guagliardi, A., Moliterni, A. G. G., Burla, M. C. & Polidori, G. (1995). *J. Appl. Cryst.* **28**, 738–744.

Artioli, G. (1997). *Nucl. Instrum. Methods Phys. Res.* B**133**, 45–49.

Attfield, J. P. (1992). *Accuracy in Powder Diffraction II*, edited by E. Prince & J. K. Stalick, *NIST Spec. Publ.* No. 846, pp. 175–182.

Attfield, J. P., Sleight, A. W. & Cheetham, A. K. (1986). *Nature (London)*, **322**, 620–622.

Audebrand, N., Auffrédic, J. P. & Louër, D. (1998). *Chem. Mater.* **10**, 2450–2461.

Balzar, D. (1992). *J. Appl. Cryst.* **25**, 559–570.

Barnes, P., Turrillas, X., Jupe, A. C., Colston, S. L., O'Connor, D., Cernik, R. J., Livesey, P., Hall, C., Bates, D. & Dennis, R. (1996). *J. Chem. Soc. Faraday Trans.* **92**, 2187–2196.

Bénard-Rocherullé, P., Louër, M., Louër, D., Dacheux, N., Brandel, V. & Genet, M. (1997). *J. Solid State Chem.* **132**, 315–322.

Bénard-Rocherullé, P., Rius, J. & Louër, D. (1997). *J. Solid State Chem.* **128**, 295–304.

Benedetti, G., Fagherazzi, G., Enzo, S. & Battagliarin, M. (1988). *J. Appl. Cryst.* **21**, 543–549.

Berg, J. E. & Werner, P.-E. (1977). *Z. Kristallogr.* **145**, 310–320.

Bertaut, E. F. (1950). *Acta Cryst.* **3**, 14–18.

Bish, D. L. & Post, J. E. (1993). *Am. Mineral.* **78**, 932–940.

Boultif, A. & Louër, D. (1991). *J. Appl. Cryst.* **24**, 987–993.

Caussin, P., Nusinovici, J. & Beard, D. W. (1988). *Adv. X-ray Anal.* **31**, 423–430.

Céolin, R., Agafonov, V., Louër, D., Dzyabchenko, V. A., Toscani, S. & Cense, J. M. (1996). *J. Solid State Chem.* **122**, 186–194.

Cernik, R. J. & Louër, D. (1993). *J. Appl. Cryst.* **26**, 277–280.

Chabre, Y. & Pannetier, J. (1995). *Prog. Solid State Chem.* **23**, 1–130.

Cheetham, A. K. (1995). *The Rietveld Method*, edited by R. A. Young, pp. 276–292. IUCr/Oxford University Press.

Cheetham, A. K. & Mellot, C. F. (1997). *Chem. Mater.* **9**, 2269–2279.

Cox, D. E. (1991). *Handbook on Synchrotron Radiation*, Vol. 3, edited by G. Brown & D. E. Moncton, pp. 155–200. Amsterdam: Elsevier Science Publishers.

Cox, D. E. (1992). *Synchrotron Radiation Crystallography*, edited by P. Coppens, pp. 186–254. New York: Academic Press.

Cox, D. E., Hastings, J. B., Thomlinson, W. & Prewitt, C. T. (1983). *Nucl. Instrum. Methods*, **208**, 573–578.

David, W. I. F., Ibberson, R. M., Matthewman, J. C., Prassides, K., Dennis, T. J. S., Hare, P., Kroto, H. W., Taylor, R. & Walton, D. R. M. (1991). *Nature (London)*, **353**, 147–149.

Delhez, R., de Keijser, Th. H., Langford, J. I., Louër, D., Mittemeijer, E. J. & Sonneveld, E. J. (1995). *The Rietveld Method*, edited by R. A. Young, pp. 132–166. IUCr/Oxford University Press.

Delhez, R., de Keijser, Th. H., Mittemeijer, E. J. & Langford, J. I. (1986). *J. Appl. Cryst.* **19**, 459–466.

Delhez, R. & Mittemeijer, E. J. (1976). *J. Appl. Cryst.* **9**, 233–234.

Dinnebier, R. E., Stephens, P. W., Carter, J. K., Lommen, A. N., Heiney, A., McGhie, A. R., Brard, L. & Smith, A. B. III (1995). *J. Appl. Cryst.* **28**, 327–334.

Dzyabchenko, A. V., Pivina, T. S. & Arnautova, E. A. (1996). *J. Mol. Struct.* **378**, 67–82.

Giacovazzo, C. (1996). *Acta Cryst.* A**52**, 331–339.

Gilmore, J. G. (1996). *Acta Cryst.* A**52**, 561–589.

Guinier, A. (1963). *X-ray Diffraction.* San Francisco: Freeman.

Harris, K. D. M., Johnston, R. L. & Kariuki, B. M. (1998). *Acta Cryst.* A**54**, 632–645.

Harris, K. D. M. & Tremayne, M. (1996). *Chem. Mater.* **8**, 2554–2570.

Hill, R. J. (1992). *J. Appl. Cryst.* **25**, 589–610.

Hill, R. J. & Cranswick, L. M. D. (1994). *J. Appl. Cryst.* **27**, 802–844.

Hill, R. J. & Howard, C. J. (1987). *J. Appl. Cryst.* **20**, 467–474.

Hill, R. J., Tsambourakis, G. & Madsen, I. C. (1993). *J. Petrol.* **34**, 867–900.

Jansen, J., Peschar, R. & Schenk, H. (1992). *J. Appl. Cryst.* **25**, 231–236.

Jenkins, R. & Snyder, R. L. (1996). *X-ray Powder Diffractometry.* New York: John Wiley & Sons.

Kitaigorodsky, A. I. (1973). *Molecular Crystals and Molecules.* New York: Academic Press.

Langford, J. I. (1978). *J. Appl. Cryst.* **11**, 10–14.

Langford, J. I. (1992). *Accuracy in Powder Diffraction II*, edited by E. Prince & J. K. Stalick, *NIST Spec. Publ.* No. 846, pp. 110–126.

Langford, J. I., Boultif, A., Auffrédic, J. P. & Louër, D. (1993). *J. Appl. Cryst.* **26**, 22–33.

Langford, J. I., Cernik, R. J. & Louër, D. (1991). *J. Appl. Cryst.* **24**, 913–919.

Langford, J. I. & Louër, D. (1982). *J. Appl. Cryst.* **15**, 20–26.

Langford, J. I. & Louër, D. (1996). *Rep. Prog. Phys.* **59**, 131–234.

Langford, J. I., Louër, D., Sonneveld, E. J. & Visser, J. W. (1986). *Powder Diffr.* **1**, 211–221.
Le Bail, A. (1992). *Accuracy in Powder Diffraction II*, edited by E. Prince & J. K. Stalick, *NIST Spec. Publ.* No. 846, pp. 142–153.
Le Bail, A. (1993). *J. Solid State Chem.* **103**, 287–291.
Le Bail, A., Duroy, H. & Fourquet, J. L. (1988). *Mater. Res. Bull.* **23**, 447–452.
Louër, D. (1992). *Accuracy in Powder Diffraction II*, edited by E. Prince & J. K. Stalick, *NIST Spec. Publ.* No. 846, pp. 92–104.
Louër, D. & Audebrand, N. (1998). *Adv. X-ray Anal.* **41**. In the press.
Louër, D., Auffrédic, J. P., Langford, J. I., Ciosmak, D. & Niepce, J. C. (1983). *J. Appl. Cryst.* **16**, 183–191.
Louër, D., Boultif, A., Gotor, F. J. & Criado, J. M. (1990). *Powder Diffr.* **5**, 162–164.
Louër, D. & Langford, J. I. (1988). *J. Appl. Cryst.* **21**, 430–437.
Louër, D., Louër, M., Dzyabchenko, V. A., Agafonov, V. A. & Céolin, R. (1995). *Acta Cryst.* B**51**, 182–187.
Louër, M., Le Roux, C. & Dubac, J. (1997). *Chem. Mater.* **9**, 3012–3016.
Louër, M., Plévert, J. & Louër, D. (1988). *Acta Cryst.* B**44**, 463–467.
McCusker, L. B. (1988). *J. Appl. Cryst.* **21**, 305–310.
McCusker, L. B. (1991). *Acta Cryst.* A**47**, 297–313.
McCusker, L. B., Grosse-Kunstleve, R. W., Baerlocher, C., Yoshikawa, M. & Davis, M. E. (1996). *Microporous Mater.* **6**, 295–309.
McCusker, L. B., Von Dreele, R. B., Cox, D. E., Louër, D. & Scardi, P. (1998). *J. Appl. Cryst.* In the press.
Madsen, I. C. & Hill, R. J. (1994). *J. Appl. Cryst.* **27**, 385–392.
Masciocchi, N. & Sironi, A. (1997). *J. Chem. Soc. Dalton Trans.* pp. 4643–4650.
Morris, R. E., Harrison, W. T. A., Nicol, J. M., Wilkinson, A. P. & Cheetham, A. K. (1992). *Nature (London)*, **359**, 519–522.
Morris, R. E., Owen, J. J., Stalick, J. K. & Cheetham, A. K. (1994). *J. Solid State Chem.* **111**, 52–57.
Newsam, J. M., Deem, M. W. & Freeman, C. M. (1992). *Accuracy in Powder Diffraction II*, edited by E. Prince & J. K. Stalick, *NIST Spec. Publ.* No. 846, pp. 80–91.
Ochando, L. E., Rius, J., Louër, D., Claramunt, R. M., Lopez, C., Elguero, J. & Amigó, J. M. (1997). *Acta Cryst.* B**53**, 939–944.
Parrish, W. (1992). *International Tables for Crystallography*, Vol. C, *Mathematical, Physical and Chemical Tables*, edited by A. J. C. Wilson, Section 2.3. Dordrecht: Kluwer Academic Publishers.
Pawley, G. A. (1981). *J. Appl. Cryst.* **14**, 357–361.
Pivan, J. Y., Achak, O., Louër, M. & Louër, D. (1994). *Chem. Mater.* **6**, 827–830.
Poojary, D. M., Cabeza, A., Aranda, M. A. G., Bruque, S. & Clearfield, A. (1996). *Inorg. Chem.* **35**, 1468–1472.
Poojary, D. M. & Clearfield, A. (1997). *Acc. Chem. Res.* **30**, 414–422.
Rietveld, H. M. (1969). *J. Appl. Cryst.* **2**, 65–71.
Rius, J. & Miravitlles, C. (1988). *J. Appl. Cryst.* **21**, 224–227.
Rius, J., Sañé, J., Miravitlles, C., Amigó, J. M., Reventós, M. M. & Louër, D. (1996). *An. Quim. Int. Ed.* **92**, 223–227.
Rius, J., Sañé, J., Miravitlles, C., Gies, H., Marler, B. & Oberhagemann, U. (1995). *Acta Cryst.* A**51**, 840–845.
Rudolf, P. & Clearfield, A. (1985). *Acta Cryst.* B**41**, 418–425.
Rudolf, P. R., Saldarriaga-Molina, C. & Clearfield, A. (1986). *J. Phys. Chem.* **90**, 6122–6125.
Runge, C. (1917). *Phys. Z.* **18**, 509–515.
Shankland, K., David, W. I. F. & Csoka, T. (1997). *Z. Kristallogr.* **212**, 550–552.
Shankland, K., David, W. I. F. & Sivia, D. S. (1997). *J. Mater. Chem.* **7**, 569–572.
Shirley, R. (1978). *Computing in Crystallography*, edited by H. Schenk, R. Olthof-Hazekamp, H. van Koningsveld & G. C. Bassi, pp. 221–234. Delft University Press.
Sivia, D. S. & David, W. I. F. (1994). *Acta Cryst.* A**50**, 703–714.
Smith, G. S. & Snyder, R. L. (1979). *J. Appl. Cryst.* **12**, 60–65.
Sonneveld, E. J. & Visser, J. W. (1975). *J. Appl. Cryst.* **8**, 1–7.
Taupin, D. (1973). *J. Appl. Cryst.* **6**, 266–273.
Toraya, H. (1985). *J. Appl. Cryst.* **18**, 351–358.
Toraya, H. (1995). *The Rietveld Method*, edited by R. A. Young, pp. 254–275. IUCr/Oxford University Press.
Valvoda, V. (1992). *Accuracy in Powder Diffraction II*, edited by E. Prince & J. K. Stalick, *NIST Spec. Publ.* No. 846, pp. 127–135.
Van Berkum, J. G. M., Delhez, R., de Keijser, Th. H. & Mittemeijer, E. J. (1996). *Acta Cryst.* A**52**, 730–747.
Visser, J. W. (1969). *J. Appl. Cryst.* **2**, 89–95.
Warren, B. E. (1969). *X-ray Diffraction.* Reading MA: Addison-Wesley.
Werner, P.-E. (1980). *Accuracy in Powder Diffraction*, edited by S. Block & C. R. Hubbard, *Natl Bur. Stand (US) Spec. Publ.* No. 567, pp. 503–509.
Werner, P.-E., Eriksson, L. & Westdahl, M. (1985). *J. Appl. Cryst.* **18**, 367–370.
Wolff, P. M. de (1957). *Acta Cryst.* **10**, 590–595.
Wolff, P. M. de (1968). *J. Appl. Cryst.* **1**, 108–113.
Young, R. A. (1995). Editor. *The Rietveld Method.* IUCr/ Oxford University Press.